Visit the Resource Center for more SIMULIA customer papers

Finite Element Analysis of Rubber Treads on Tracks to Simulate Wear Development

Sergio G. Arias, Ph.D.

Advanced Technology Group, Camoplast Solideal Inc.

Abstract: FEA applications to conduct product development at Camoplast Solideal, Inc. have been implemented to understand better the rubber track behaviors. Numerous simulation studies have already been conducted on the rubber tracks to understand their strengths and limitations. An important study is now being pursued to the development of a tool that will help us understand better the wear mechanisms happening on the treads of our rubber tracks. These rubber tracks are normally used for agriculture applications, and determining wear or useful lifetime properties of the treads is a difficult task. Obtaining empirical data to model the wear of the tread is difficult, as proven by our field test where ground surface interactions are difficult to characterize. This paper will describe the process of simulating the mechanism of wear that occur at the treads when a track is rolled over a surface. The objective of this research is to obtain an analytical procedure, validated with field tests that will help us understand better the conditions that affect rubber erosion at the treads to develop new rubber tread designs.

Keywords: Rubber simulation, cyclic fatigue, tread design, wear, FEA, friction.

1 Introduction

Any structural component that is in motion, of affected by the motion of others, will always suffer from a performance decline due to the phenomenon of wear development. This is supported by the 1st and 2nd Laws of Thermodynamics which state that all energy is conserved in a system and that no system can be perpetually in motion. When a system is in motion, the kinetic energy used to generate its motion will be transformed in other forms of energy. Wear is a consequence of some of this energy change, which ultimately will cause the system to fault.

The study of wear has been conducted for many years, and numerous definitions can be found in literature. In material science, wear is defined as the material degradation generated in the contact surfaces of the material as two solid bodies are sliding or rolling.

Although this is true for most cases, wear is not limited to contact between two solid bodies. Wear, as in the form of erosion, can be found in the contact of a solid body with a moving fluid (such as water or air). Additionally, it is important to mention that corrosion or fracture of structural components is not considered a form of wear since both of these failure mechanisms can happen even if there is no relative motion between parts, and they do not require contact between two bodies to exist. Instead, they could be produced with the presence of wear. Hence, wear can be described in a more generic definition, as the progressive damage caused by the relative motion of two contact surfaces, which will generate a loss of material or produce a change in geometry, if allowed to progress without limit.

1.1. Fundamentals of Mechanical Wear

The presence of wear and how it evolves varies enormously depending upon many factors. Lubrication, loading and environmental conditions, such as time, temperature and erosion agents can affect the development of wear. But among these factors, the type of material in the contact bodies will be a critical factor in the contribution of friction, and consequently the development of wear.

Wear mechanisms of a structural component can be thought in general as the failure mechanisms of its material occurring near or at the surface contact by the relative motion of other components. Most material failure mechanisms can be described in terms of brittle fracture, fatigue, plastic deformation, etc. In

general, development of wear can occur in the mechanism described in Table 1. But in practice, however, wear processes tend to use more than just one mechanism. As a consequence, it is generally difficult to test wear for a specific mechanism.

Table 1. Most common wear mechanisms found in rubber-like materials

1. Adhesion wear
2. Single-Cycle Deformation
3. Repeated-Cycle Deformation
4. Oxidation
5. Thermal
6. Abrasion
7. Others (fretting, erosion, etc.)

For the research conducted in this paper, the type of wear that is of most interest to us is that of rubber-like materials. According to some researchers, rubber wears by two main mechanism; tearing (fracture) and fatigue. In both mechanisms, they arise from high local friction effects at or near the contact surface. These areas can be characterized into two areas of interest, as seen in Figure 1: the Interfacial wear zone and the cohesive wear zone. Depending upon some key material properties, such as the tensile strength of the rubber, one would obtain different mechanism and rates of wear developing at these areas.

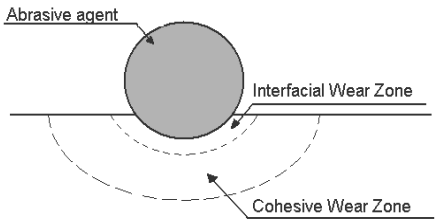

Figure 1 - Schematic of wear zones in a typical rubber-like material

The wear development found typically in the rubber tracks of caterpillar-drive systems is that of abrasion and Repeated-Cycle Deformation. Abrasion wear is caused mainly at the cohesive wear zone by hard particles or other erosion agents.

In a repeated-cycle deformation, the wear mechanism requires repeated cycles of deformation to cause failure. This wear mechanism is too found at the cohesive wear zone. In these types of processes, the plastic strain is accumulated, nucleating more and more cracks and propagating them throughout the cycles, to the point of fracture. This is symptomatic of cyclic fatigue wear. The following figure shows a schematic of this wear development.

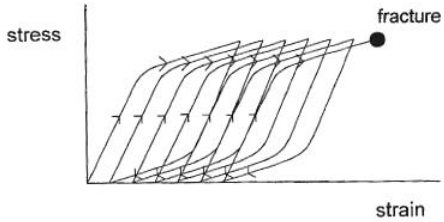

Figure 2 - Illustration of repeated stress cycling leading to fracture

In a typical repeated-cycle wear, the wear scarring produced is varied, depending upon inherited material properties (hardness of rubber, strength, yielding etc…) and of course, the contact pressure. In practice, no matter how small the pressure load or contact stress is, because sufficient rolling or sliding will generate

this type of fatigue wear. This type of mechanical wear is very typical in rolling and impact wear situations and it is found in all the rubber tracks of caterpillar-drive systems.

1.2. Case Study: Abnormal wear on rubber track

As mentioned earlier, wear studies are of considerable importance when parts made of rubber are directly involved in the motion of any structural assembly, as in the case of the caterpillar track system. There are many other factors that contribute to the failure of these parts, but unlike most of them, the wear of rubber components is generally complex to predict.

For the purpose of this research, the case of the abnormal wear development in the rubber tracks of a caterpillar-type vehicle was selected. Figure 3 shows an schematic of the assembly of a typical positive-drive rubber track agriculture vehicle.

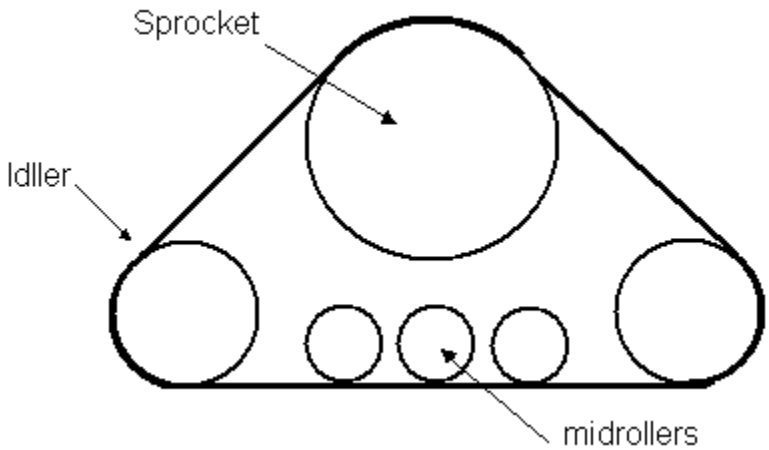

Figure 3 – Schematic of a typical positive-drive rubber track system

Field studies showed that the tracks produced localized areas of wear in the treads, even after only several hours of use. These areas of abnormal wear, which are clearly defined as seen in Figure 4, are located in the inside part of the contact area of treads with the ground surface (away from the region of pressure induced by the midrollers). The reason why this occurs is not clear, since logic dictates the treads should either wear nearly evenly or where most contact pressure occurs. The following figure shows an example of a typical wear tread on a harvest combined vehicle track.

Figure 4 - Localized tread wear

In order to obtain a better understanding in these phenomena, Camoplast Solideal, Inc. decided to conduct an experimental field test that will focus on the study of the development of this abnormal wear. The procedure of this experimental testing will be described next.

2 Experimental Testing

As mentioned earlier, an unusual localized tread wear has been found in our rubber tracks after just several hours of use. These areas of wear diminish the performance of the track (ie. traction performance) long before the track ends its usefulness life. A significant field study was conducted to give light to the phenomena of the development of this localized tread wear.

Upon visual examination on the rubber tracks, it was clear that the areas of high wear were perfectly defined to be in the sections away from the roller path. In other words, the high wear was located at the inside areas of the treads. The areas where the midrollers passed by, as the vehicle rolls, showed minimal wear, and more consistent to what is expected to deteriorate the treads after hours of use.

To study more closely this phenomenon, a camera was rigged in cage with a glassy surface such that it would record the deformations of the treads as the undercarriage system of the vehicle rolled over it. The following figure shows the setup created to conduct these experiments.

Figure 5 - Field Testing Setup to measure tread deformation

To produce a clearer visual measure of the tread behavior as the midroller passed them by, a discretized mesh was drawn over several treads (as seen in Figure 6). This field testing setup provided us with sufficient visualization of the mechanisms of tread deformation.

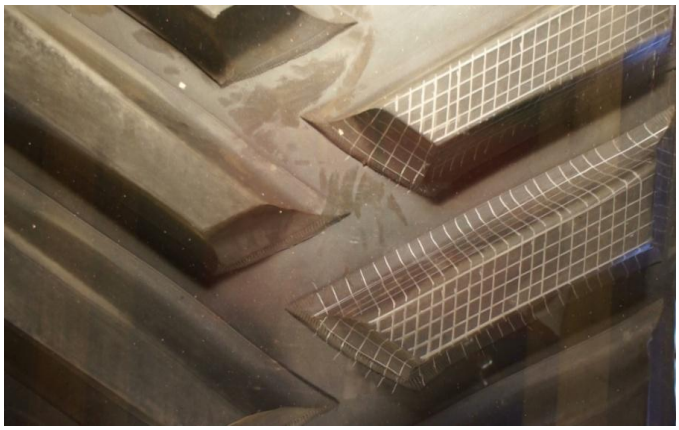

Figure 6 - Field testing visual observation set up

3 FEA Model Description and Material Characterization

The methodology typically used for testing carcass solicitation is that of the "waterbug" test setup (as seen in Figure 7). In this type of setup instead of simulating the entire vehicle or the undercarriage track system, the model simulates only the behavior of a section of the track where the midrollers roll over. Since, it is believe the midrollers are the undercarriage components that carry the highest and most critical loads to the track.

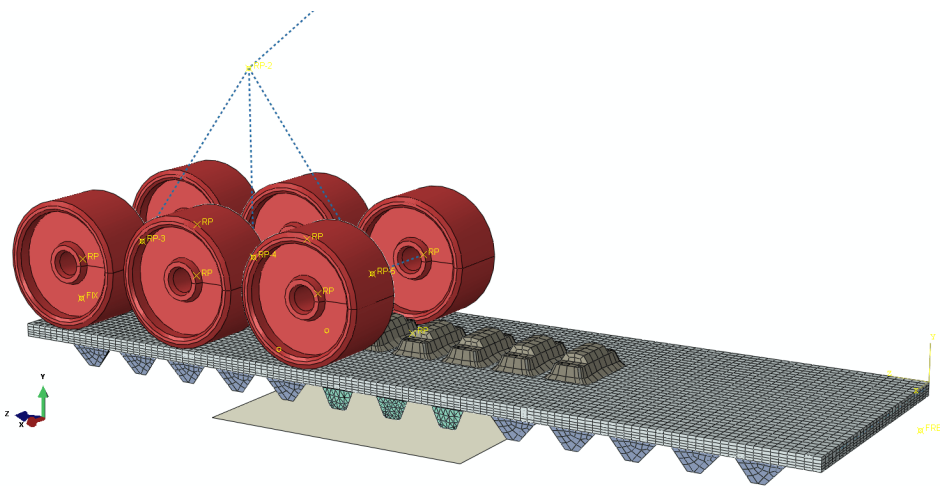

Figure 7 – Abaqus model for the Waterbug simulation test setup

In order to ensure that this model depicts with authenticity the behavior of what happens in the field, certain procedures must take place. First, the section modeled needs to have the proper track tension that will see in the field. In order to do that, the track section is given a 0.1% elongation, which will represent the proper tension. That is, the track is fixed in one end to have U_x, U_y and U_z equal to zero, meanwhile the other (free) end is given a U_z displacement of 0.001*Length.

The length of the track section was taken arbitrarily. It must be long enough to accommodate the midroller assembly and the consequent rolling over. For this simulation, the length was equal to 2,232-mm.

To have a track that simulates correctly the rigidity and flexibility of the track, the FEA track model must have all the structural components. Additionally, other main components of the undercarriage assembly must be properly modeled. The components used in the FEA simulations are:

1. Carcass
2. Drive Lugs
3. Treads
4. Reinforcement layers (modeled only the 0-degree)
5. Midrollers
6. Undercarriage (UC)
7. Ground

The undercarriage (UC) component which encompasses extremely rigid members was modeled using beam-type connectors. A hinge connector was modeled as well to simulate the kinematics of the pivot point of the entire UC sub-assembly. Then, all midrollers were linked to the UC by means of hinge and beam connectors. The Midrollers were modeled using analytically rigid regions. The rubber layer in the midrollers was assumed to cause negligible difference for this simulation case.

All rubber parts were modeled using hybrid elements. The carcass and lugs were modeled using linear hexahedral reduced elements, C3D8RH. The carcass was portioned into several areas to create a finer mesh

around the point of interest (the center of the track), and the lugs were only modeled at the center of the track to reduce computational time.

The chevrons, or treads, were modeled into two groups. Those treads away from the center of the track were modeled with using C3DR8H with a coarse mesh, with their geometric properties simplified to allow the use of hexahedral elements. A group of six treads, with the exact geometric definitions, located at the center of the track were modeled using linear tetrahedral elements C3D4H, with a finer mesh. The reason behind this modeling approach was to model, as accurate as possible the treads in the track without causing too much computational time.

The 0-degree reinforcement was the only layer included in this simulation. It was assumed that the bias angled layers provided little difference in the outcome and hence were taken out in the modelization of the reinforcement of the track. This was done as well to reduce computational time. The 0-degree reinforcement layer was modeled using membrane-type elements, M3D4R. The rebar section properties were defined to match the actual 0-degree layer found on the field tracks. The ground was modeled using an analytical rigid component.

The problem size of this simulation produced a total number of 116,743-elements, and close to 360,000 degrees of freedom. Table 2shows in detail the information for all the components used in the simulation. The fourth columns shows the material types used for each component, which indicates what type of rubber compound was used for its definition (this will be shortly explained in the next section).

Table 2. Information of the Finite Element Analysis model

Components	Element Type	# of elements	Material Type	Material Model
Chevrons (centered,6)	C3DH	23,744	Rubber B	Van der Waals
Ground Surface	Analytical Rigid	-	-	-
Midrollers (6)	Analytical Rigid	-	-	-
Layer_o-deg	M3D4R	1,628	Rubber C, Steel	Marlow
Carcass	C3D8RH	19,470	Rubber A	Van der Waals
Chevron (away,20)	C3D8RH	322	Rubber B	Van der Waals
Drive Lug (6)	C3D8RH	108	Rubber D	Odgen, N=5
UC connectors	Beam(6), Hinge (4)	10	-	-

It is important to note that the ground was modeled to influence only the central six treads, and not the entire track. The reasoning behind this was to reduce the computational time that would create having the total 26 tread interactions with the ground surface. Instead, the treads away from the center of the track would have the U_y degree of freedom to be constricted, and allow free movement in the other directions. It is assumed that this would not cause much influence in the behavior of the central six treads, which would give us the accurate data.

The simulations were conducted on a dual quad-core computer (3GHz processor, 16GB of RAM, 300GB HDD), using Windows XP 64-bit. The software version was Abaqus 6.11. The solver made use of the parallelization capabilities and 7 cores were used in the solution process. The estimated CPU usage time per simulation was approximately 80,000-sec, or 22 hours. This turns out to be approximately 4.6-hours, wallclock time.

3.1. Material Characterization

The material model characterization will be discussed in this section. A total number of 5 different materials were used in the finite element analysis model. Aside of steel used for the cables as part of the

reinforcement, 4 different rubber compounds are used for the manufacturing of the main track components, and are labeled as rubber compound type A, B, C or D.

These rubber compounds will generally have different intrinsic properties that were designed to obtain the best mechanical properties for the purpose of its component. Rubber compound A, for instance, is the compound used for manufacturing of the carcass, and therefore has rubber properties (ie, flexibility, rigidity, rolling resistance, etc) best fitted for its use. Rubber compound B and D are the materials used for the construction of the treads and drive lugs, respectively. Due to the nature of the function of these track components, these compounds are generally stiffer than that of rubber compound A, for instance. Rubber compound C is used as the adhesion compound for the reinforcement of the rebar layers.

All these rubber compounds were characterized by a third party (AXEL Products, Inc.), and the stress-strain curves were generated to define their properties in terms tension, planar and bi-axial loadings. Each compound was pre-strained and then, a series of loading cycles were conducted to match the strain ranges at which they are stressed when they are used in the field tests. Then, they were evaluated with Abaqus software to find the proper hyperelastic model to fit their particular characteristics. Table 1 showed all the different hyperelastic models used for their modelization.

4 Results and Discussion

On this section, we will discuss the results found on the finite element analysis and how its output solution relates to the phenomena of the abnormal wear which was found in the field studies. Additionally, we will discuss the mechanism of this particular wear based on the visual inspection done on the laboratory at the Centre de Technique de Camoplast.

4.1. Microscopic Inspection of the tread wear

Two treads specimens were extracted out of a track in which the abnormal tread wear had occurred during the field test: One tread from the left side and another one from the right side of the tread design of the track. The following figure shows the top-view of the treads used for this visual inspection. The Optical microscope, by Lumenera Infinity 3 was used for this visual analysis process.

Figure 8 - Left side and Right side treads, with the severe worn areas marked in white, and the less worn areas marked with an "X"

After cleaning the excessive debris, they were carefully inspected under an optical microscope to observe the wear pattern in the two distinctive surfaces found on the treads. The following photos show the typical wear patterns found at the outer-sides of the tread contact areas (the area marked with an “X”).

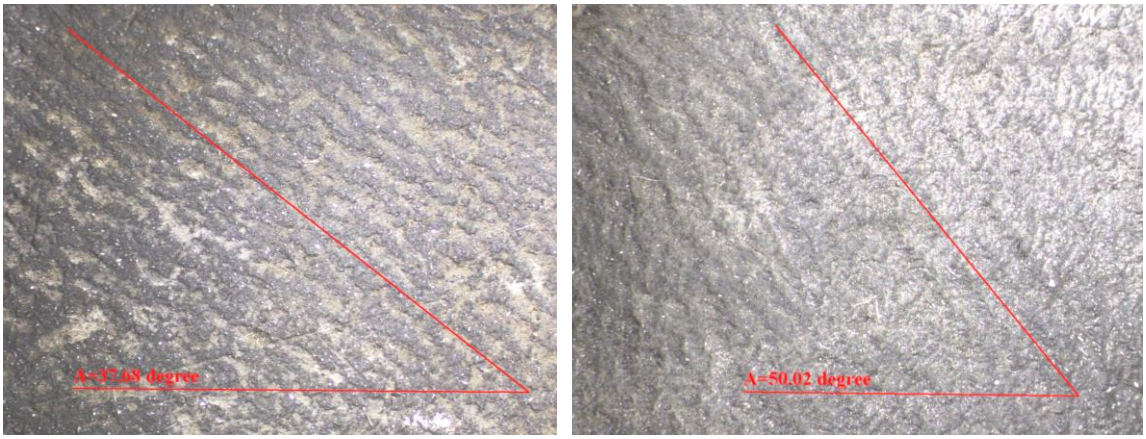

Figure 9 - Typical wear pattern for a left side tread, at the center location (left) and outer location (right) at the less worn area of the tread

The wear pattern at this surface was clearly very rough. There were found a lot of areas in this region depicting the abrasive type wear. But additionally, we could see indications of striation patterns in its surface. Optical measurements of the distance between the striations were in the order of 0.85-mm. to 0.92-mm. Another interest conclusion taken from this close-up visualization is the angle upon which these striations were formed, and how it varied in position within the contact patch. As it is shown in Figure 9, the striation orientations varied between approximately 50-degree to 30-degrees with respect to the longitudinal length of the tread, as it approached the more severed worn areas.

The following photo shows a detail image of the wear at the center of the abnormal wear area of the same tread (the area marked in white, in Figure 8). Optical measurements of the striations were between 0.12-mm to 0.20-mm. approximately. And the angle of these striations was clearly more parallel with the longitudinal length of the tread, with angles around 12-degrees. This worn area was very smooth, and these striations were hardly noticeable.

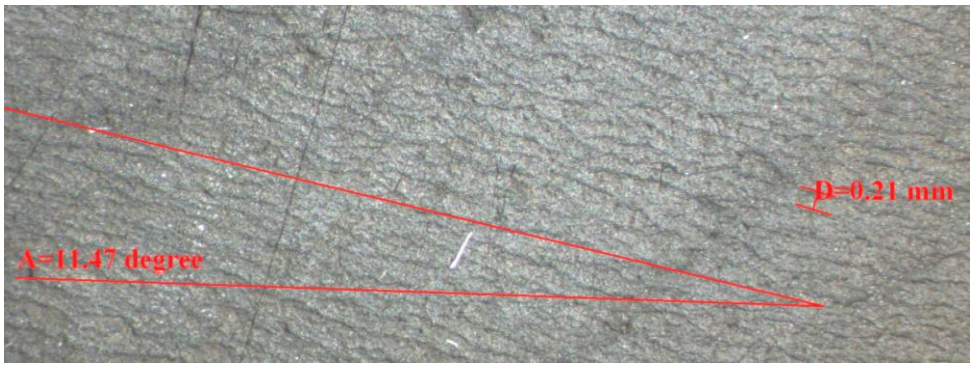

Figure 10 - Closed up wear pattern of a typical, severe worn area

A similar wear pattern was found to be in the other tread, but since it belonged to the other side of the track, its wear characteristics was just a mirrored copy of the left-side tread. This tells us that the wear mechanism was indeed symmetric, with its plane of symmetry right at the center line of the track width.

The following image shows a schematic of how the wear pattern was found in these two treads. Note how the striation geometry is very similar in both treads, and how it is mapped symmetrically by the center of the track width.

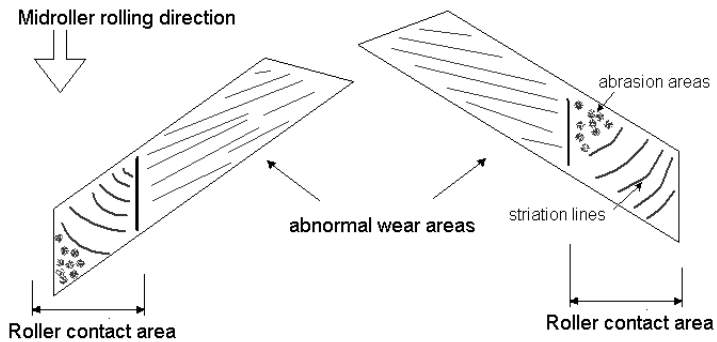

Figure 11 - wear pattern schematic found on the two inspected treads

4.2. Finite Element Analysis Results

As it was explained earlier, the FEA model was fixed in such a way where one end is fixed and the other one is given a predetermined displacement, which creates the tension that is felt by the track when it is in placed in the undercarriage system. The following pictures shows how this tension was measured, using the 0-degree layer (which is assumed to carry most of the load) as our basis of measurement. The rebar forces were measured at the center of the layer, via a nodal path. This was done to avoid edge effects found at both ends of the track. As it can be seen a total from this picture, a total of 14,000-lbf was observed. In later analysis, the displacement condition was reduced in order to bring back the tension of the track to the more realistic value of 10,000-lbf.

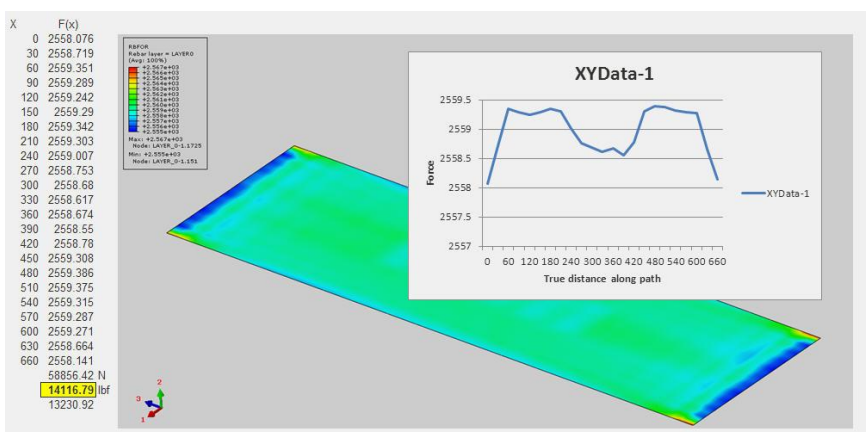

Figure 12 - RBFOR, rebar forces at 0-deg layer

A total of three steps were simulated. The first step in the simulation was, as mentioned earlier, the tensioning step, where the free end of the track is giving a 1% stretch of its length (in this case, 2.2-mm.). Additionally, a downward displacement was induced in the undercarriage system to enforce contact of the midrollers with the rubber track surface. Then, in the second step a downward load is placed at the center of

gravity of the undercarriage (UC). This was done to represent the weight of the, subsequently sinking the six rollers further into the track. The third and final step (via implicit dynamics) forces the UC system to move 1000-mm. along the length of the track, for the period of 1-sec.

Output of the simulation was recorded in terms of contact results (CPRESS, CSHEAR, and CSLIP).The following picture shows the CPRESS distribution (contact pressure) plot when the middle roller is precisely lying in top of the middle tread bar. The CPRESS represents the magnitude of the normal force at the contact nodes.

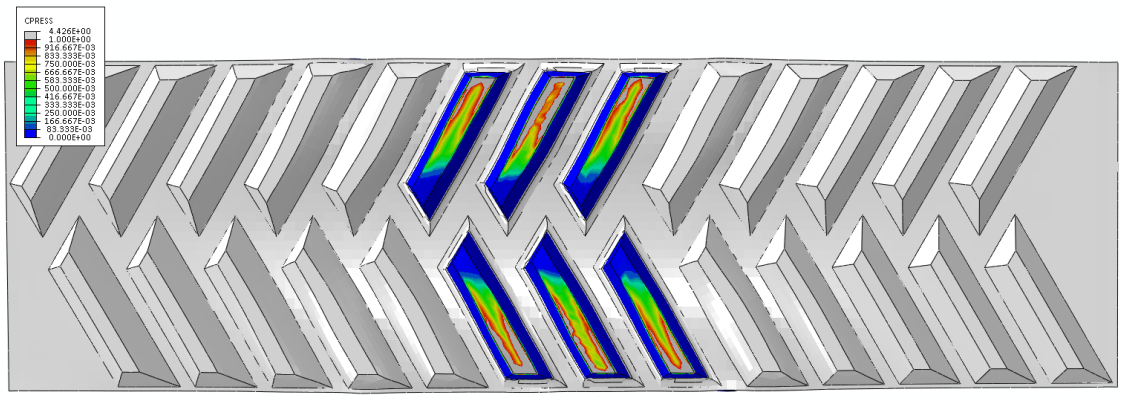

Figure 13 – CPRESS distribution; contact pressure

As it can be seen from this image (for ease of display, the upper and lower limits were set to ±5MPa), the pressure is mostly distributed along the tread bar area in which the midrollers pass by This tells us that the tread bar pressure is not constantly distributed along its contact surface, but rather, that is proportional to the width of the rollers which induces the deformation of the tread bar.

When we look at the contact nodal displacement, as the roller passes by, we noticed that the longitudinal (direction of roller displacement) nodal position remains consistent, throughout the bar contact surface. That is, that there is no much difference in the displacement (direction of motion) of a contact node, regardless of its place in the contact surface. But, the same cannot be said of their transverse displacement. The next figures show the transverse contact nodal displacement, CSLIP1.

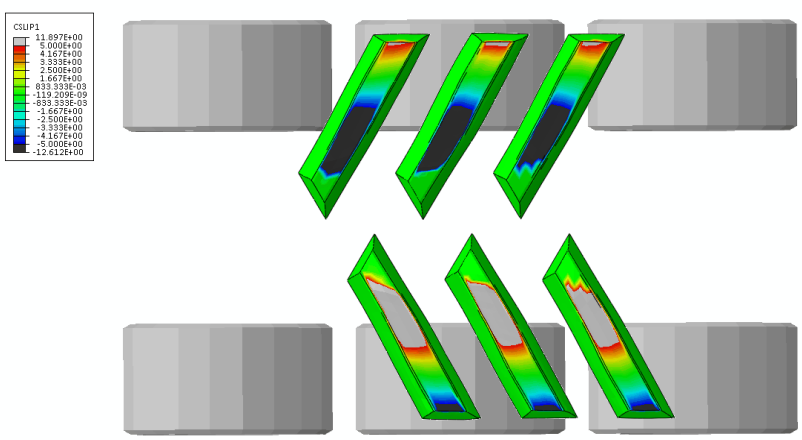

Figure 14 – CSLIP1 distribution; transverse nodal displacement

In this image, we can see how much a contact node displaces, normal to the direction of motion. The CSLIP1 shows the regions where most transverse displacement occurs (in the areas of black and grey colors), which in this case happens to be away from the CPRESS areas, the roller width section.

This tells us that the reason for the localized wear of the tread bars, at this particular section, has to do with the transverse motion that the tread bar suffers as the rollers passes by, and not by the directional motion of the tread bar. As a consequence, we can deduct that the wearing of material is mostly induced by the transverse frictional shearing of the tread bars. The following figure shows the CSTATUS, and tells us what areas of the contact are in slipping conditions (in green color).

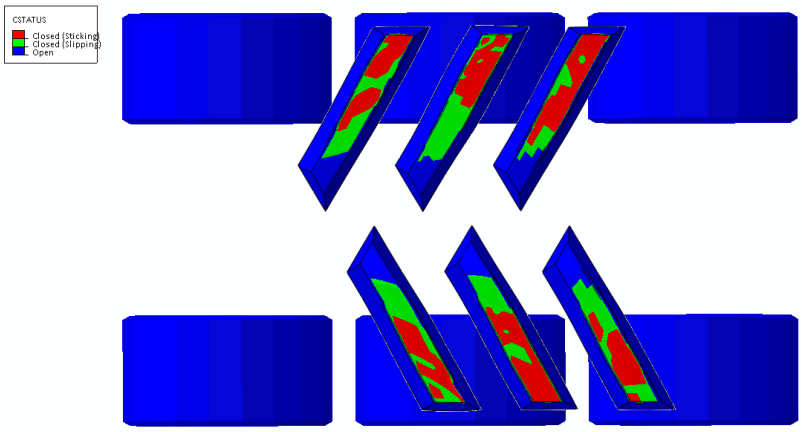

Figure 15 – CSTATUS, contact characteristics at the tread bars

5 Conclusion

It is concluded from this research that based on the visual inspection in the field test, and supported by the microscopic examination that the variation of the tread wear in the track is due to a significant change in contact and loading mechanisms at the ground-to-tread area. We found that the severe wear happens in the region which is away from the midroller influence (the region with supposedly less pressure). Closer visual inspections told us that the wear mechanism at these two areas was consistently different. These surfaces were different in terms of roughness and striation properties. The severely worn areas exhibited very smooth surfaces, with small striations indicating high fatigue wear. The areas under the midroller influence showed little fatigue wear (large striations), and the normal abrasion type wear you would expect in these mechanical conditions.

The finite element analysis simulations provided us with a look at how the contact pressure was distributed as the midrollers passed by. The simulation model also gave us a mapping of the slip and shearing conditions at the ground to tread contact areas. We were able to see that the areas within the midroller influence suffered from very little slip and shear –friction forces, due to the high pressure values. On the other hand, there was large transverse slip nodal displacement at the area with poor contact pressure. These areas are therefore prone to the high cyclic fatigue wear found in the field studies.

6 References

1. Briscoe, B., "Wear of Polymers: an Essay on Fundamental Aspects", 3rd International Conference on the Wear of Materials, San Francisco, USA, 1981.
2. Ludema, K. C., "Friction, Wear, Lubrication: a Textbook in Tribology", CRC Press, 1996.
3. Bayer, R. G., "Mechanical Wear Fundamentals and Testing", 2nd Edition, Revised and Expanded, Marcel Dekker, Inc., 2004.
4. Bauman, J. T., "Fatigue, Stress, and Strain of Rubber Components. A Guide for Design Engineers", Hanser Publishers, Munich, 2008.
5. Gent, A. N., "Engineering with Rubber. How to Design Rubber Components", 2nd Edition, Hanser Publishers, Munich, 2001.
6. Bekesi, N. "Friction and Wear of Elastomers and Sliding Seals", Budapest University of Technology and Economics, Budapest, 2011.
7. Baek, D. K., Khonsari, M. M., "Friction and Wear of a Rubber Coating in Fretting", Elsevier B.V. Publishers, 2004.